Nonlinear Optics for Frequency-Doubling in Nanosatellite Laser Communication

Jim Clark
Massachusetts Institute of Technology, Space Systems Laboratory
Bldg. 37-350, (617) 253-8541
jimclark@mit.edu

Faculty Advisor: Kerri Cahoy
Massachusetts Institute of Technology, Space Systems Laboratory

ABSTRACT

Free-space optical communication attracts interest due to its promise of higher data rates for similar size, weight, and power costs compared with radio systems. However, while satellite-to-ground optical communication has been tested from low Earth orbit and the Moon, intersatellite optical links are still an area of active research and development. Second-harmonic generation (SHG, or "frequency doubling") with nonlinear optics may improve the link margins of laser systems that serve as crosslinks as well as downlinks. For example, the output of a 1550 nm laser could be doubled to 775 nm on command, allowing the satellite to use whichever wavelength is advantageous (e.g. improved detector and propagation properties), without spending the mass budget for an entire second laser system. Link-budget analysis suggests that a nanosatellite crosslink can gain 3-4 dB of link margin with a frequency-doubler. This improvement is largely driven by the reduction in beamwidth that comes with the higher frequency. It is not substantially greater than the improvement that comes with using the same narrower beamwidth at 1550 nm. However, SHG would allow a diffraction-limited system to use different beamwidths for beacon acquisition and communication without any moving parts.

INTRODUCTION

Free-space optical communication (a.k.a. laser communication or lasercom) has been attracting interest due to its promise of higher data rates for similar resources compared to radio systems. The potential of lasercom is derived from the Friis link budget equation:

$$P_{rx} \propto P_{tx} \frac{A_{rx} A_{tx}}{\lambda^2 R^2} \qquad (1)$$

Transmitted power (P_{tx}) and transmitter area (A_{tx}) are constrained by the limits of a spacecraft's size, weight, and power budgets (especially for increasingly-popular nanosatellites), receiver area (A_{rx}) is constrained by platform resources, and transmission path distance (R) is constrained by the spacecraft's mission and orbit. Incremental gains can be made in these variables and in other limiting factors (efficiency, sensitivity, etc.), but the only "lever" available for orders of magnitude of improvement is wavelength (λ). The six orders of magnitude of improvement that comes with changing from radio (millimeters-squared) to optical (micrometers-squared) can be used to increase data rate and reduce the size and cost of receivers and transmitters. Space-to-ground tests have shown great promise, such as the demonstration of 622 Mbps from the Moon to four 40-cm telescopes with superconducting nanowire single-photon detectors (SNSPDs) on Earth with the Lunar Laser Communication Demonstration.[1]

Small satellites are especially constrained by available transmit power and aperture size, which has resulted in proposed CubeSat missions to demonstrate optical communication technologies in small form factors. The Optical Communication and Sensor Demonstration (OCSD) by The Aerospace Corporation[2] and the Nanosatellite Optical Downlink Experiment (NODE) by MIT[3] are two such missions, proposing to demonstrate downlink data rates of tens of megabits per second from LEO. NODE in particular is leveraging the availability of commercial off-the-shelf optical communication hardware from the terrestrial telecom industry: seed lasers and amplifiers intended for fiber optic communication are being assembled in a compact form factor for use in space.

As free space optical communication on space platforms becomes more widespread, the availability of receivers will become a limiting factor for data capacity. NODE is developing a small low-cost optical receiver as part of its effort, and companies such as BridgeSat[4] are developing global networks of optical receivers.

Constellations of satellites can also take advantage of cross-links to reduce downlink latency, as satellites which are over ground stations can serve as relays to their siblings which are not. However, satellites face more restrictions on their receiver architecture. There are plans from BridgeSat, NASA, and other agencies to construct multi-meter aperture telescopes on the ground, but small satellite platforms cannot physically accommodate such large receive apertures. LLCD's receiver used a cryogenically-cooled detector, but it is unlikely for cryogenic cooling to be widespread on CubeSat platforms.

The design space of nanosatellite optical communication can be expanded by the incorporation of a frequency-doubling nonlinear optical element, which may improve the received power margins of crosslinks while remaining simple and low in cost. We propose the development and testing of a frequency-doubling optical transmitter (FDOT) for nanosatellites. FDOT would allow satellites to use commercial off the shelf (COTS) fiber optic communication parts and remain compatible with existing and planned optical receiving stations, and also have the ability to transmit at visible wavelengths on demand to improve the link margin of intersatellite crosslinks.

Nonlinear Optics

Nonlinear optical materials are the key to the functionality of FDOT. Most materials exhibit a nearly-linear response to applied electrical fields. However, some materials exhibit nonlinear responses when excited to high field intensities, such as by focused lasers. One such nonlinear optical process is second-harmonic generation (SHG), in which laser light of a particular wavelength passes through a carefully manufactured nonlinear crystal and is converted to light of half the incoming wavelength, for example, 1550 nm to 775 nm. Periodically-poled lithium niobate (PPLN) is a commonly-used material for doubling the wavelengths of interest to optical communication (~1 micrometer). An illustration of the inputs and outputs of a crystal of PPLN doubling 1550 nm light is shown in Figure 1.
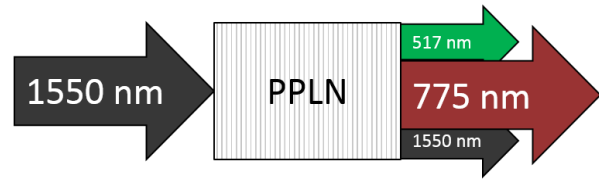

Figure 1: Second Harmonic Generation (SHG) in Periodically-Poled Lithium Niobate (PPLN)

Note that most light is doubled to 775 nm, but that some 1550 nm light passes straight through, and some parasitic third-harmonic generation at 517 nm is also occurring.

One critical element of second-harmonic generation (and any nonlinear process in which multiple frequencies are present) is phase-matching. The index of refraction of a material is dependent on wavelength, and so as light passes through a material and undergoes SHG, the input light and the second harmonic move at different speeds and so become out of phase with each other and destructively interfere in a matter of micrometers (called the coherence length). In some materials, such as PPLN, this phase mismatch is neutralized by quasi-phase matching. The crystal is exposed to electromagnetic fields during manufacturing that cause the nonlinear optical coefficients to form domains of opposite signs. This causes the second harmonic to alternate between being faster and slower than the input wave, causing them to remain in-phase on average and maximizing conversion efficiency. This process is illustrated in Figure 2, a diagram from Thorlabs (a manufacturer of nonlinear optical crystals and other optical components).[5]

The poling period must be carefully controlled, and depends on the wavelength being doubled. If the phase mismatch is not incremented and decremented by the same amount over alternate poling domains, then the phase mismatch will eventually grow enough to result in destructive interference. In practice, crystals can be manufactured with multiple tracks of different poling periods for different wavelength ranges, and thermal control can be employed to expand and shrink the crystal and its poling for further adjustment.
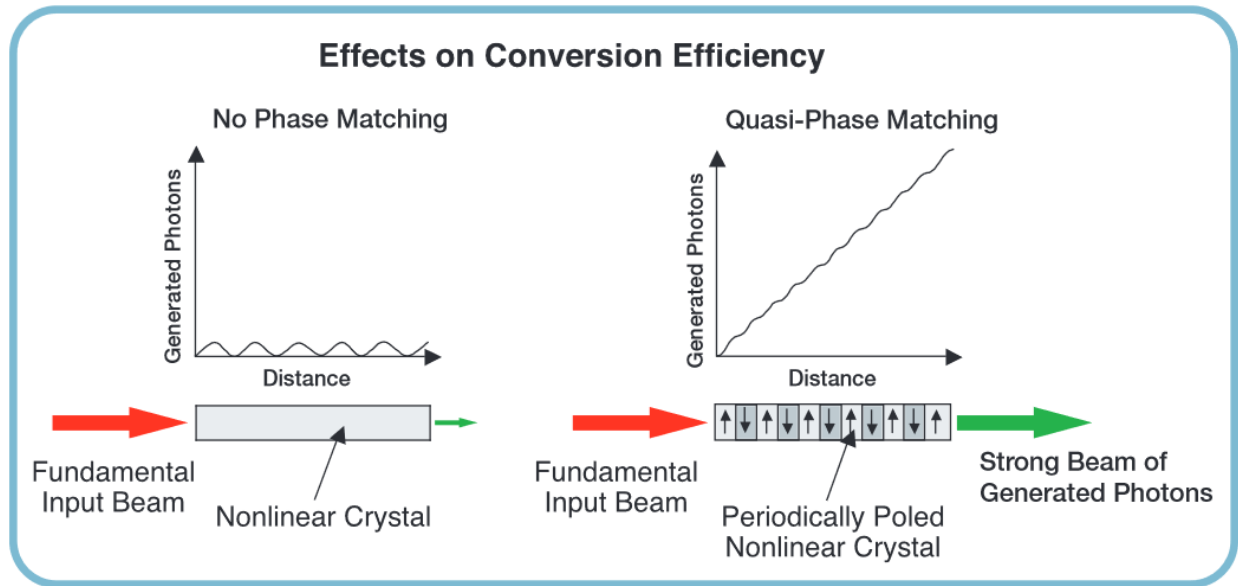
Figure 2: An Illustration of the Effect of Periodic Poling and Quasi-Phase Matching on SHG Conversion Efficiency.[5]

GomX-2 was a CubeSat carrying SPEQS, an optical parametric oscillator (a "frequency-halver"), to demonstrate a different nonlinear process which has applications for quantum key distribution. GomX-2 was unfortunately lost when the launch vehicle failed catastrophically.[6]

Avalanche Photodiodes

One of the advantages of links at 775 nm is that the APDs used in optical receivers at that wavelength have better noise properties than the APDs used to detect 1550 nm.

APDs are photodiodes with a reverse bias voltage applied, so that when photons encounter the semiconductor and excite individual electrons, an easily-detected "avalanche" current is produced.[7] The semiconductors and architectures used for APDs are selected based on the wavelengths and bandwidths of interest; for example, indium gallium arsenide (InGaAs) is used for infrared wavelengths (800-2500 nm)[8], and silicon is used for visible and near-infrared wavelengths (200-1200 nm).[9]

One of the noise sources of APDs is "excess noise", which scales with the APD gain M_{APD} and a factor k_A which depends on the semiconductor (0.02 for silicon, and 0.45 for InGaAs)[10].

$$F_A = k_A M_{APD} + (1 - k_A)(2 - 1/M_{APD}) \qquad (2)^{11}$$

This excess noise grows faster than gain does, so for some received power on the detector, there is an ideal gain which maximizes signal-to-noise ratio (SNR). Because silicon APDs have a lower k_A than InGaAs, their excess noise is lower and they can be operated at higher gains. Typical APD gains are around 10 for InGaAs and 100-150 for silicon.[10] The optimum gain for a given material and received power is calculated by Equation 3:

$$M_{APD,opt} = \left(\frac{4k_b T}{q(I_l + I_{dg}) \times R_L} \right)^{1/(2+x)} \qquad (3)^7$$

Where k_B is the Boltzmann constant (1.38×10^{-23} J/K), T is the APD temperature (K), q is the elementary charge (1.602×10^{-19} C), and x is an empirically-determined excess noise coefficient for an APD architecture (0.3 for silicon, 0.45 for InGaAs[10]. It is distinct from k_A; where k_A is used in the exact formulation of excess noise in Equation 2, x is used in an approximation $F_A \approx M_{APD}^x$ which is more amenable to differentiation. This approximation is used to derive the optimum APD gain.[7]

I_l and I_{dg} are the photocurrent produced by incident photons (at unity gain, or $R_{APD}P_{rec}$) and dark current subjected to gain, respectively. (There is also I_{ds}, dark current which is not subject to gain, but because the APDs are operated at gains much greater than 1, it is negligible.)

The dark current and responsivity are parameters of the specific APD. For this analysis, two APDs were selected as being generally applicable for optical communication and having readily accessible datasheets: the InGaAs G8931-04[8] and the silicon S12023-10[9]. The optimum gain curves are plotted in Figure 3 (with the G8931-04 plotted alone in Figure 4, for visibility).
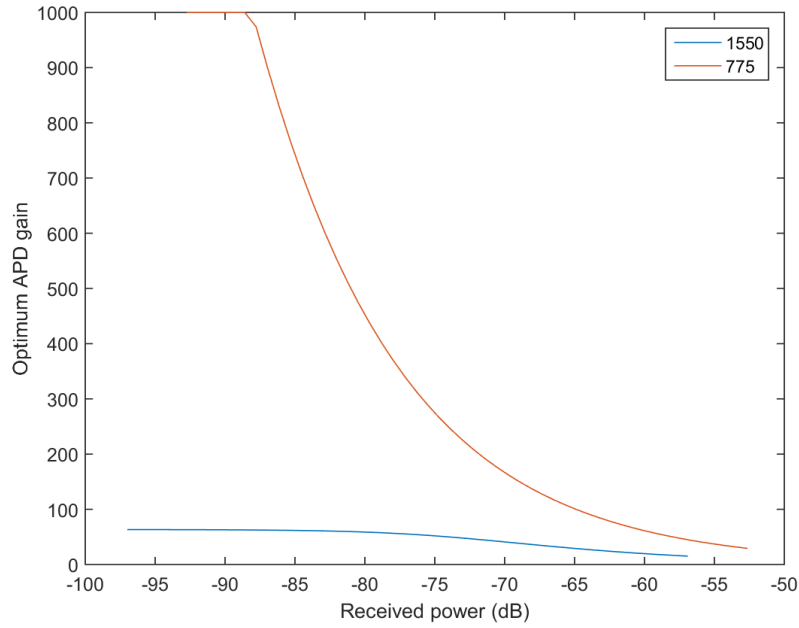

Figure 3: Optimum gain vs. received power for silicon APD S12023-10 (red) and InGaAs APD G8931-04 (blue).
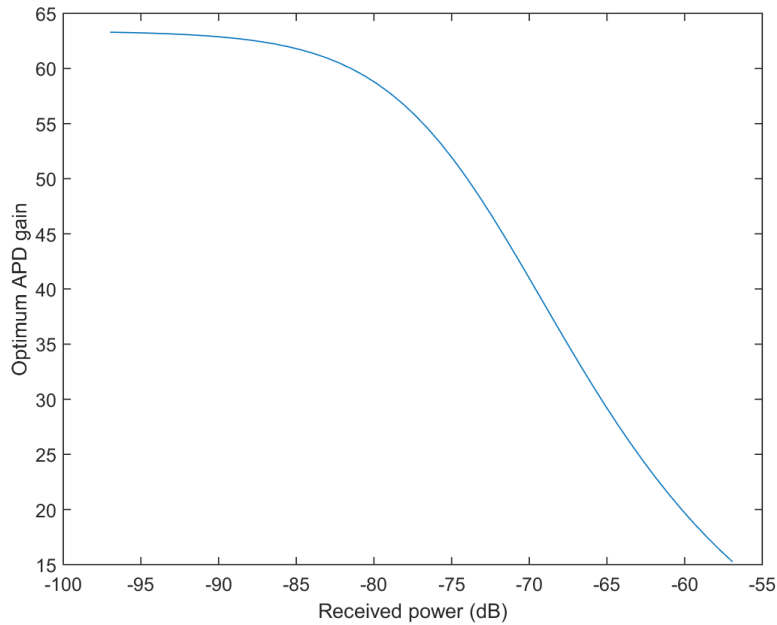

Figure 4: Optimum gain vs. received power for InGaAs APD G8931-04 (magnified to show detail).

FREQUENCY-DOUBLING OPTICAL TRANSMITTER

The concept of operations of the frequency-doubling optical transmitter (FDOT) is that a satellite will include an optical transmitter made of COTS parts operating at the standard optical communication wavelength of 1550 nm, with the addition of a frequency-doubling nonlinear optical element to have the capability to transmit on two different wavelengths using a common seed laser, modulator, and amplifier (as opposed to doubling its communication system's mass, power, and volume by carrying an entire second laser system). A block diagram illustrating the system in two modes of operation is shown in Figure 5. At the top, the nonlinear element is inactive, and the 1550 nm laser passes through unmodified. In the second mode, the element is active and doubles the light passing through it to 775 nm. Such a system has been proposed and studied at JPL (including participation by the author) for interplanetary exploration missions[12], but the author presently considers the utility of such a system for nanosatellites.
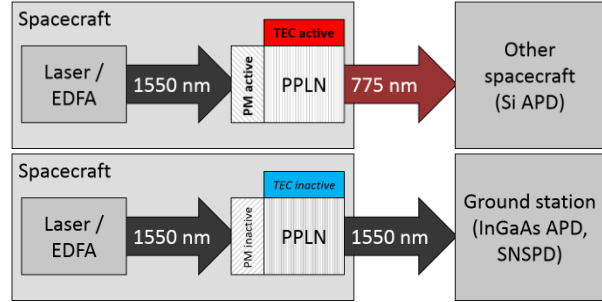

Figure 5: An Illustration of a Frequency-Doubling Optical Transmitter in Two Modes of Operation.

The advantage that this approach has is that it allows a system to use the best features of each frequency for the situations in which they are favored, for less than the mass of having one conventional system for each. One such trade, considering 1550 nm and 775 nm with a PPLN doubler, is laid out in Table 1. There are many other trades to be made, both in terms of materials and frequencies to be used, such as Potassium Titanyl Phosphate (KTP) and 1064/532 nm, and in terms of system architecture, such as the choice of linear-mode APDs, Geiger-mode APDs, or superconducting nanowire single photon detectors.

Table 1: A brief qualitative trade to motivate the utility of frequency-doubling optical transmitters.

	1550 nm	775 nm	Hybrid
Positive	COTS telecom hardware available and inexpensive Lower photon energy means more photons generated, reduced shot noise	Silicon APDs have less thermal noise than InGaAs[10,11] Narrower diffraction limit	Takes advantage of the positives of both wavelengths
Negative	Most ground stations use cryogenic cooling to reduce detector noise, challenging to implement on CubeSats	Falls within FAA definition of "visible" – extra reg. overhead to downlink[13] Most current and planned ground stations operate at NIR, e.g. OCTL[14], LLGT[15], and BridgeSat (based on AeroCube[16]) Greater sky radiance at visible wavelengths (ground stations only)[17]	Conversion is not 100% efficient
Mass (est.)	200 g (MOPA)[3], laser parts only	100 g (HPLD, max bandwidth < 100 MHz)[3]	200 + 65 g (MOPA + PPLN, polarizer, optics)

The key to the functioning of this system is that PPLN and other frequency-doublers can be controlled by temperature and polarization. A crystal will only double a narrow range of frequencies depending on its poling period, and thermal expansion is exploited to allow a crystal's center frequency to be tuned. Some empirical data which illustrates this effect, from an experiment conducted by the author and Bill Farr, is shown in Figure 6.

Even if the poling period is matched to the frequency, only light which is polarized perpendicular to the crystal axis of PPLN can be doubled. If the polarization is switched to be at parallel to the crystal axis, no doubling will occur.

In either case, it is possible to implement the switching with no moving parts, for some power cost. Crystal

ovens intended for laboratory use require several watts to operate[18]. This can be improved in the space environment, but the power cost of a polarization-switcher, being a simple electro-optical component, is more straightforward to calculate. Therefore, the FDOT studied here is assumed to use a crystal whose poling period is such that it doubles 1550 nm light (with a thermoelectric cooler to maintain the crystal's center frequency when SHG is being performed), and a polarization switcher is used to move light into and out of the polarization state that is doubled. This is possible because NODE (and FLARE, it is assumed) use pulse-position modulation, which allows the laser light to be of one polarization. For polarization-modulation systems, two crystals at right angles to each other would be required, and the operating point of the crystals would have to be moved well away from the ambient temperature of the spacecraft.
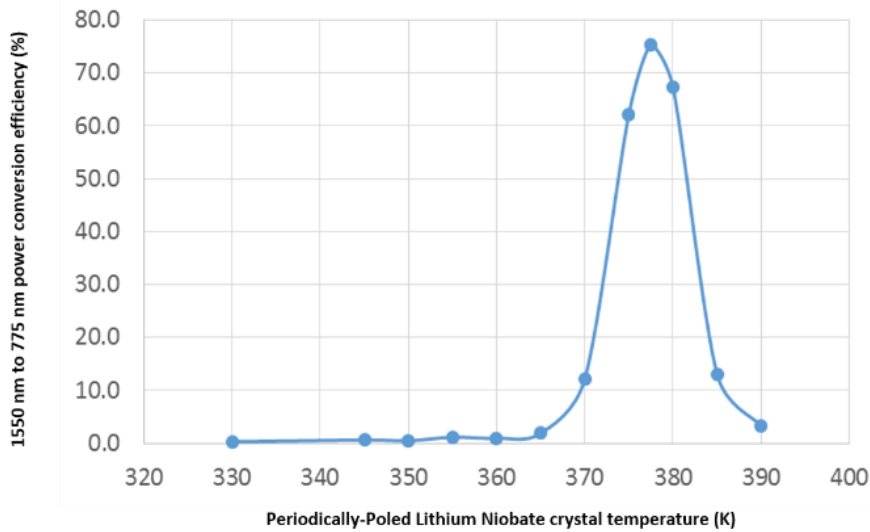

Figure 6: SHG Conversion Efficiency vs. Temperature for a PPLN Crystal.

A major focus of this research has been to develop tools to explore the laser communication trade space expanded by this option and determine where improvements of at least 3 dB in link margin and/or data rate over state-of-the-art 1550 nm links can be obtained.

DESIGN SPACE EXPLORATION

Link budgets for direct-detected laser communication with pulse position modulation (PPM) do not behave in the same way as link budgets for radio communication. Moision and Xie have developed an approximate channel capacity equation that incorporates the three major constraints on a lasercom channel: signal power, noise power, and finally, the modulation bandwidth itself.[19] These constraints are represented in order by the

terms in the denominator of the channel capacity equation.

$$C_{OPT} \approx \frac{1}{E \ln 2} \left(\frac{P_r^2}{P_r \frac{1}{\ln M} + P_n \frac{2}{M-1} + P_r^2 \frac{MT}{E \ln M}} \right) \quad (4)$$

For NODE and other links where the received signal power is on the order of hundreds of photons-per-bit, the predominant constraint is the third, where the channel capacity is capped by the bandwidth of the laser modulation (the slot rate and PPM order). In such circumstances, it is most helpful to calculate the margin of received power with respect to the minimum required power to distinguish pulses at that slot rate and PPM order above the noise from the detector and the sky, with some desired bit error rate.

The design space exploration tool used for this research is based on link-budget analysis performed by Ryan Kingsbury for his thesis[3] and extended by Emily Clements to analyze the sensitivity of the link margin to variations of several input parameters (paper submitted)[20]. The author incorporated the option of frequency doubling. The frequency-doubling analysis tool performs two parallel analyses for the two cases: a baseline case at 1550 nm, and a second case at 775 nm, which takes into account the loss of electrical power to the laser due to the oven or polarization switcher, the loss of laser power due to conversion inefficiency, the different noise and gain characteristics of silicon vs. InGaAs avalanche photodiodes (APDs), and the different sky background noise at 1550 and 775 nm (where applicable).

Case study: FLARE

The Free-space Lasercom And Radiation Experiment (FLARE) is a mission under development at MIT composed of two CubeSats which will, among other tasks, demonstrate a laser crosslink at a tentatively planned range of 200 km. The current design includes an 85-mm receive aperture and a 1550 nm laser transmitter based on COTS telecom hardware.[21] An early revision of the satellite, with its receive aperture front and center, is depicted in Figure 7.
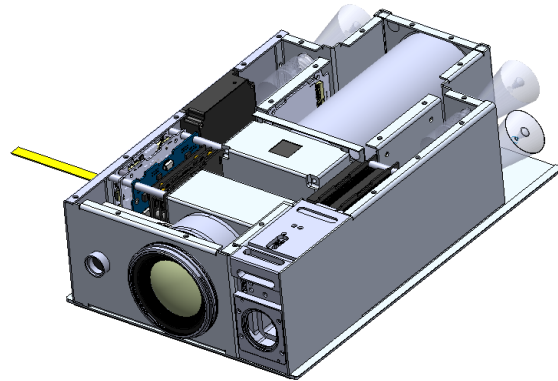

Figure 7: Cutaway Diagram of FLARE.[21] Dimensions: 10 x 20 x 30 cm. The receive aperture depicted is an 85 mm *f*/1.8 camera lens. This is not the final design of FLARE, but will be used as the notional design for all analyses.

For the simulation, the PPM order and slot rate have been set to typical values from NODE (order 64, 200 MHz). The electrical power budget of the laser communication system was varied from 5 to 50 W to encompass the range typified by NODE (8 W)[3] and OCSD (56 W).[2] The link range was varied from 100 km to 10,000 km (approximately $1/3^{rd}$ of the distance to GEO) to capture the closest and most distant encounters that could reasonably be expected in LEO. Atmospheric background noise and transmittance were not included, although they are different for the two wavelengths: per Hemmati[17] Table 8.16, background noise is 4×10^{-4} W/cm^2-sr-μm at 1550 nm and 7×10^{-3} W/cm^2-sr-μm at 775 nm. Per Table 8.13, surface-to-space transmittance is 97% at 1550 nm and 91% at 775 nm. This is an item for future work.

A contour plot of the resulting differences in margins – in other words, the link margin at 775 nm minus the link margin at 1550 nm – is shown in Figure 8. At FLARE's current design point (5.7 W electrical, 200 km range), the improvement in margin is -1.1 dB.
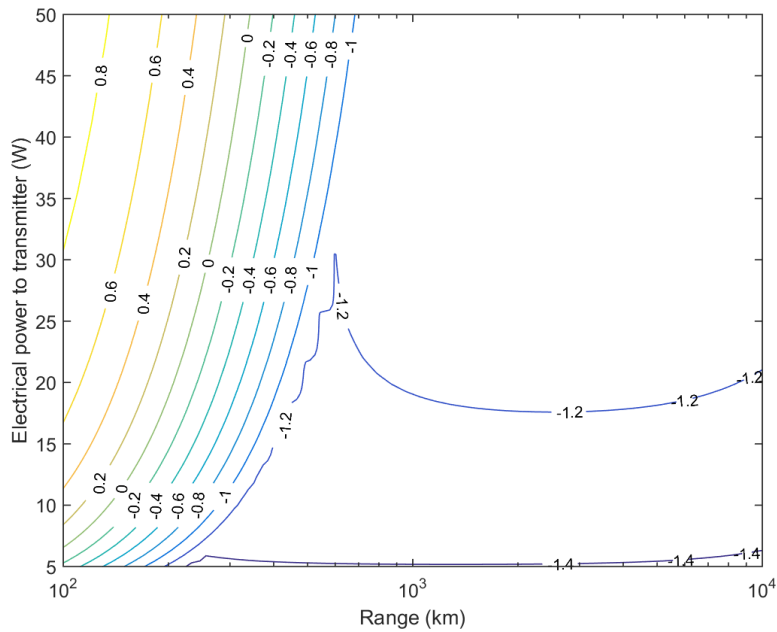
Figure 8: Improvement in FLARE's optical link-budget margin with collimation-limited optics and frequency-doubler (dB). The distortion of the -1.2 dB contour is a MATLAB artifact from the discrete test points and reduced rate of change.

For most of the design space studied, the link margin was reduced. The reason for the large region between the -1 and -1.2 dB contours (i.e. the reason that the contours do not continue indefinitely towards the right side of the graph) is that silicon gain tops out at 1000 (the maximum recommended by the datasheet[9]) and InGaAs gain tops out at 63.4.

Case study: Diffraction-limited FLARE

FLARE's transmit beamwidth is determined by a collimator, while the beamwidth of a diffraction-limited system is proportional to λ/D, which improves by a factor of 2 with SHG (thus improving gain by a factor of 4, or 6 dB). During a conversation with Bill Farr, it was suggested that a second case should be run to capture this improvement. For this case study, the system was assumed to have an aperture diameter of 1.67 mm, which produces a 2.26 mrad wide (HPBW) diffraction-limited beam at 1550 nm. A contour plot of the resulting differences in margins is shown in Figure 9. At FLARE's current design point (5.7 W electrical, 200 km range), the improvement in margin is 3.0 dB.
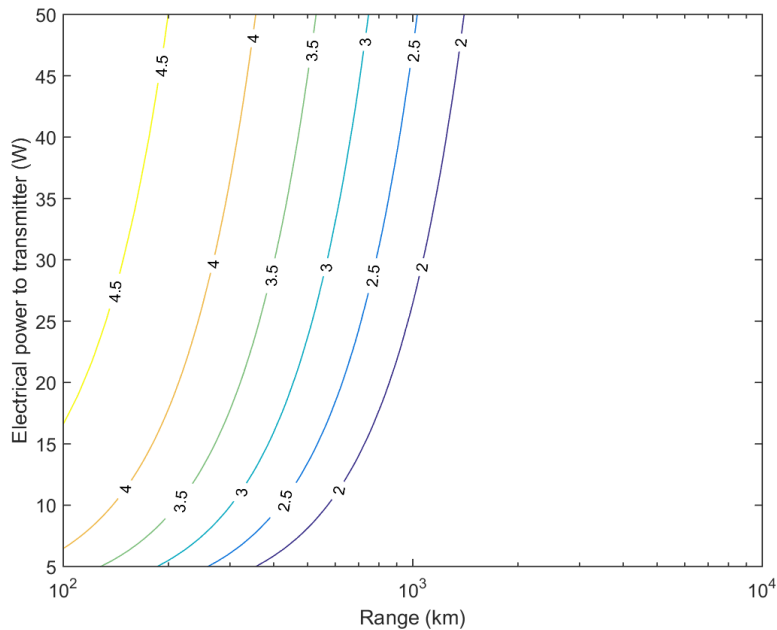
Figure 9: Improvement in FLARE's optical link-budget margin with frequency-doubler (dB), diffraction-limited case.

We are seeing the lower-bound on the link budget improvement from SHG identified in the first case. It is shifted to longer ranges, as the higher received power from the extra 6 dB of transmitter gain keeps the optimum silicon APD gain below 1000 for longer. However, we are also beginning to see that there is a maximum improvement as well. To probe that phenomenon, a third case study was performed with a narrower beamwidth, to produce higher received optical power.

Case study: Diffraction-limited 2 cm aperture

The 2.26 mrad beamwith of NODE (assumed to be used for FLARE) was selected on the basis of being as wide as possible while supporting a 10 Mbps link at a range of 1,000 km to a 30-cm aperture on a 10 W input power budget[3]. However, narrower beams are achievable, such as the 15-microradian downlink beam used by LLCD.[15] A beam of the order of 100 μrad would require a diffraction-limited transmit telescope with a larger aperture. A 2 cm aperture, producing a beamwidth of 189 μrad, is physically achievable in a CubeSat, but would challenge the two-stage pointing found to be necessary to enable the fine pointing that NODE requires. However, a dedicated gimbal assembly of the required accuracy could be supported by a 100-kg microsatellite. For example, the NFIRE-LCT had a pointing error of approximately 170 μrad[22] and a mass of 35 kg[23]. A contour plot of the resulting differences in margins is shown in Figure 10. At FLARE's current design point (5.7 W electrical, 200 km range), the improvement in margin is 4.0 dB.
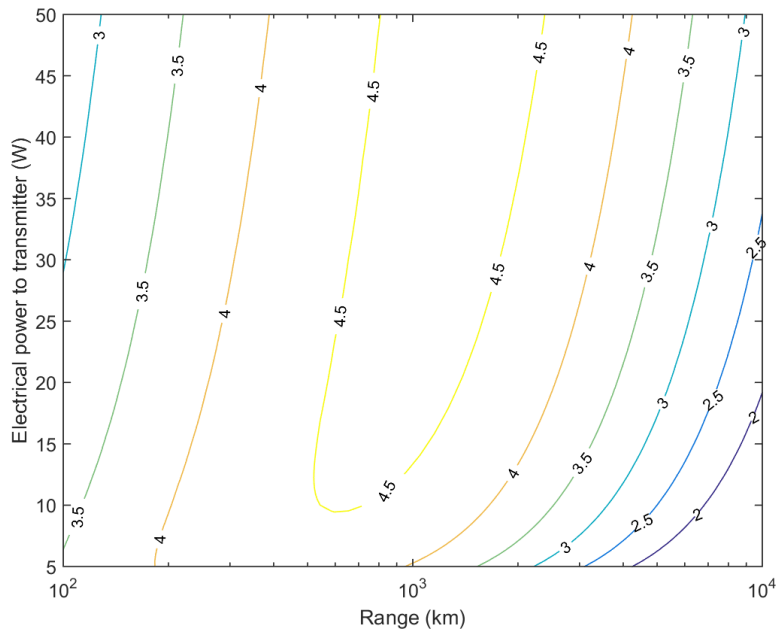
Figure 10: Improvement in 2 cm diffraction-limited optical link-budget margin with frequency-doubler (dB).

This case shows a notable peak where FDOT is maximally effective, with a decrease in performance at closer and further distances. The limiting factor at close range is shot noise. The shot noise of an APD depends on received photon flux and on its gain, and at close ranges, silicon's optimum gain flattens out while the optimum gain on InGaAs continues to fall.

Case study: Half-angle FLARE

Because some of the improvement in link margin from SHG comes from the 6 dB increase in received power from reducing the beamwidth by a factor of 2, a fourth case was run to examine the impact of simply reducing the beamwidth of FLARE (i.e. comparing 2.26 mrad to 1.13 mrad) while staying at 1550 nm. A contour plot of the resulting differences in margins is shown in Figure 11. At FLARE's current design point (5.7 W electrical, 200 km range), the improvement in margin is 3.3 dB.

At long ranges, where APD gain is maximized and constant in both cases, the 6 dB improvement is reduced by the dependency of shot noise on the square root of received power. At close ranges, the received power is high enough that the APD gain can be reduced, which reduces shot noise relative to the amount of power received and further improves SNR and the link margin improvement.
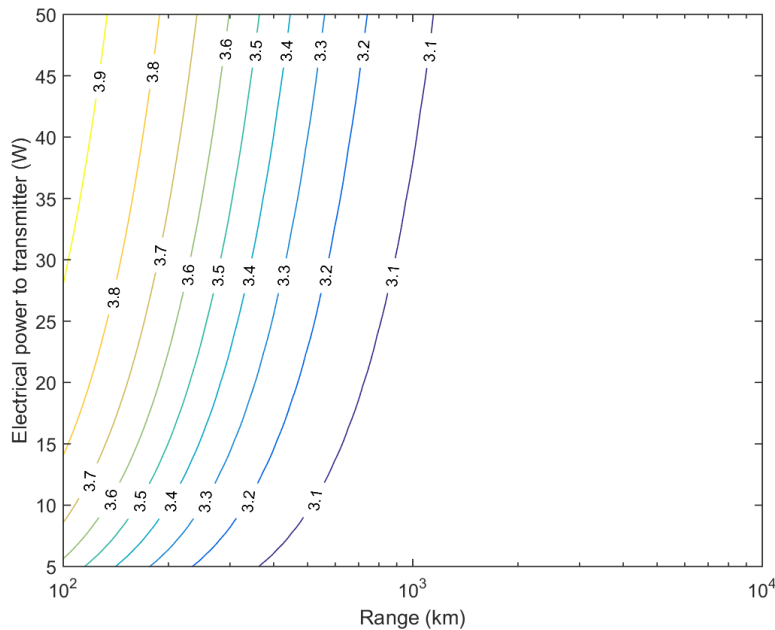
Figure 11: Improvement in collimator-limited FLARE optical link-budget margin by halving the beamwidth (dB).

Future work

Many of the terms in the link budget analysis tool are dependent on the specific detector diode chosen and other details of the optical receiver. A component-level sensitivity analysis will be performed. Other case studies will be performed for different mission, transmitter, and detector architectures, including lunar nanosatellite missions similar to MIT's KitCube project.[24] SHG can also be used to allow an infrared communications laser to generate visible wavelengths suitable for calibrating scientific telescopes, to fulfill proposed satellite guide-star concepts.[25] Alternate nonlinear optical processes, such as optical parametric oscillation, will be studied to develop methods for nanosatellites to use their communication systems to generate longer wavelengths suitable for atmospheric science[26,27] or frequency combs[28].

CONCLUSION

We have analyzed the effects of a frequency-doubling nonlinear optical element on FLARE, a planned nanosatellite experiment to demonstrate an intersatellite crosslink in LEO. With the system as-designed, the link margin is reduced by -0.86 dB. However, when applied with a diffraction-limited system, the link margin can be improved by 3-4 dB. A similar improvement can be obtained more simply, by narrowing the beamwidth of the 1550 nm laser by a factor of 2, but using SHG allows the beam to be widened or narrowed on-demand without

moving parts, which may be useful for adaptive beacon-tracking or responding to changes in spacecraft pointing capability. The developed design space exploration tool can be applied to other regimes, such as lunar nanosatellites, and non-communication applications, such as extending nanosatellite optical communications systems to be useful for photometric calibration and atmospheric science.

REFERENCES

[1] Murphy, D. V., Kansky, J. E., Grein, M. E., Schulein, R. T., Willis, M. M., and Lafon, R. E., "LLCD operations using the Lunar Lasercom Ground Terminal," 2014, p. 89710V–89710V–7.

[2] Janson, S., and Welle, R., "The NASA Optical Communication and Sensor Demonstration Program," *AIAA/USU Conference on Small Satellites*, Aug. 2013.

[3] Ryan Kingsbury, "Optical Communications for Small Satellites," Massachusetts Institute of Technology, 2015.

[4] "Products - Satellite data collection, bandwidth, ground network services," *BridgeSat Inc.*

[5] Thorlabs, *Periodically Poled Lithium Niobate (PPLN) - Tutorial*.

[6] Cheng, C., Chandrasekara, R., Tan, Y. C., and Ling, A., "Space qualified nanosatellite electronics platform for photon pair experiments," *arXiv:1505.06523 [physics, physics:quant-ph]*, May 2015.

[7] Hamamatsu, *Characteristics and use of Si APD (Avalanche Photodiode)*.

[8] Hamamatsu, "InGaAs Photodiodes Selection Guide," Mar. 2015.

[9] Hamamatsu, "Si APD (Avalanche Photodiode) Selection Guide," Mar. 2014.

[10] Excelitas Technologies, *Avalanche photodiode: A User Guide*.

[11] Govind P. Agrawal, "Optical Communication Systems (OPT428)."

[12] William Farr, and John Hamkins, "Frequency Agile Optical Communications Laser," Aug. 2014.

[13] Federal Aviation Administration, "Order JO 7400.2K: Procedures for Handling Airspace Matters," 2014.

[14] Oaida, B. V., Wu, W., Erkmen, B. I., Biswas, A., Andrews, K. S., Kokorowski, M., and Wilkerson, M., "Optical link design and validation testing of the Optical Payload for Lasercomm Science (OPALS) system," 2014, p. 89710U–89710U–15.

[15] Boroson, D. M., Robinson, B. S., Murphy, D. V., Burianek, D. A., Khatri, F., Kovalik, J. M., Sodnik, Z., and Cornwell, D. M., "Overview and results of the Lunar Laser Communication Demonstration," 2014, p. 89710S–89710S–11.

[16] The Aerospace Corporation, "2015 Annual Report" Available: http://www.aerospace.org/publications/annual-reports/2015-annual-report/.

[17] Hemmati, H., ed., *Near-Earth Laser Communications*, CRC Press, 2009.

[18] Covesion, "PV Oven Series," 2015.

[19] Bruce Moision, and Hua Xie, *An Approximate Link Equation for the Direct-Detected Optical PPM Link*, 2014.

[20] Emily Clements, "Notes on NODE Link Budget Analysis with Uncertainty and Sensitivity Analysis," Mar. 2016.

[21] Kerri Cahoy, "FLARE: Free-space Lasercom and Radiation Experiment."

[22] Fields, R., Kozlowski, D., Yura, H., Wong, R., Wicker, J., Lunde, C., Gregory, M., Wandernoth, B., and Heine, F., "5.625 Gbps bidirectional laser communications measurements between the NFIRE satellite and an Optical Ground Station," *2011 International Conference on Space Optical Systems and Applications (ICSOS)*, 2011, pp. 44–53.

[23] Heine, F., Kämpfner, H., Czichy, R., Meyer, R., and Lutzer, M., "Optical inter-satellite communication operational," *MILITARY COMMUNICATIONS CONFERENCE, 2010 - MILCOM 2010*, 2010, pp. 1583–1587.

[24] "KitCube | Taking CubeSats farther than ever before."

[25] Albert, J., "Satellite-mounted Light Sources as Photometric Calibration Standards for Ground-based Telescopes," *The Astronomical Journal*, vol. 143, 2012, p. 8.

[26] Schweitzer, S., Kirchengast, G., and Proschek, V., "Atmospheric influences on infrared-laser signals used for occultation measurements between Low Earth Orbit satellites," *Atmos. Meas. Tech.*, vol. 4, Oct. 2011, pp. 2273–2292.

[27] Andreas Fix, Christian Büdenbender, Martin Wirth, Mathieu Quatrevalet, Axel Amediek, Christoph Kiemle, and Gerhard Ehret, "Optical parametric oscillators and amplifiers for airborne and spaceborne active remote sensing of CO_2 and CH_4," *SPIE Remote Sensing*, International Society for Optics and Photonics, 2011, pp. 818206–818206.

[28] Boggio, J. M. C., Moro, S., Windmiller, J. R., Zlatanovic, S., Myslivets, E., Alic, N., and Radic, S., "Optical frequency comb generated by four-wave mixing in highly nonlinear fibers," *2009 Conference on Lasers and Electro-Optics and 2009 Conference on Quantum electronics and Laser Science Conference*, 2009, pp. 1–2.